

Microstructures of TC21 alloys after hydrogenation and dehydrogenation

Xiao-li WANG¹, Yong-qing ZHAO², Xiao-wei WEI¹, Hong-liang HOU³

1. School of Material Science and Engineering, Xihua University, Chengdu 610039, China;
2. Northwest Institute for Nonferrous Metal Research, Xi'an 710016, China;
3. Beijing Aeronautical Manufacturing Technology Research Institute, Beijing 100024, China

Received 27 May 2013; accepted 12 November 2013

Abstract: Microstructural evolution and phase transformation of hydrogenated and dehydrogenated TC21 alloys were investigated by optical microscopy (OM), X-ray diffraction (XRD) and transmission electron microscopy (TEM). XRD peaks of α and β phases after hydrogenation shifted to low angle because of lattice expansion with the solution of hydrogen atoms. Microstructure of TC21 alloy after hydrogenation changed apparently. Compared to the as-received one, the contrasts of equiaxed α phase and transformed β phase under optical microscope were reversed. In addition, XRD and TEM analyses revealed that hydrides and α' martensite precipitated from α and β phases. Bulk of twins and some Ti_3Al particles were observed in hydrogenated TC21 alloy, which means that hydrogen led to the redistribution of alloying elements in α and β phase. After dehydrogenation, the microstructure of TC21 alloy was similar to that of the as-received one, which consisted of α and β phases.

Key words: δ hydride; Ti_3Al phase; α' martensite; twin

1 Introduction

Ti–6Al–2Sn–2Zr–3Mo–1Cr–1Nb (TC21) alloy is a new α/β high strength and toughness alloy as a candidate material for structural parts of advanced aircraft [1–3]. However, high cost of machining attributed to low limit of deformation, high deformation resistance, high flow stress, low strain rate and high hot working temperature is the bottleneck of large scale application. In recent years, thermohydrogen processing (THP) has been proved to be an effective way to modify microstructures and enhance the mechanical properties and processability of titanium alloys. It has been shown that the addition of hydrogen increases the ductility, reduces the flow stress and decreases β transformation temperature of titanium alloys [4–6]. ZONG et al [7] reported that the addition of 0.3% (mass fraction) hydrogen in Ti–6Al–4V alloy decreased the flow stress by 11.2% and increased the plasticity by 20%, which was attributed to the following reasons: hydrogen induced the decrease of stacking fault energy and dislocation density; the occurrence of twinning in starting microstructure; the increase of more

workable β phase; dislocation mobility and stimulated evolution of dynamic recrystallization during hot working. CHEN et al [8] investigated the effect of hydrogen on high temperature yield strength of Ti-60 alloy. The experimental results showed that high temperature yield strength of Ti-60 alloy continuously decreased with increasing hydrogen contents, and it reduced about 70% at 900 °C for the alloy containing 0.3% hydrogen. HE et al [9] studied the deformation behavior of Ti40 alloy after hydrogenation and reported that the flow stress initially increased and then decreased with the increase of hydrogen content because of solution strengthening by hydrogen and precipitation of new phase. The superplastic forming and diffusion bonding (SPF/DB) of hydrogenated TC21 alloys were carried out by WANG et al [10] and the results showed that the bonding ratio increased with hydrogen. ZONG et al [11] studied the effects of hydrogen addition on high temperature deformation behavior of TC21 alloy and the results showed that suitable hydrogen addition can significantly decrease the flow stress and improve the hot workability of TC21 titanium alloy.

The change of microstructure and precipitation of

hydrides plays an important role in mechanical properties and working properties of titanium alloys. The addition of hydrogen leads to precipitation of new phases and generation of defects in specimens [12–15]. In this work, the effects of hydrogen content on precipitation of new phases and generation of defects are investigated, which is beneficial to further research on mechanical properties and working properties of titanium alloys.

2 Experimental

The received TC21 titanium alloy consisting of α and β phases was used. The bars of TC21 alloy were heated to 900 °C, held for 1 h and cooled in air to room temperature. Specimens with the size of $d10 \text{ mm} \times 20 \text{ mm}$ were directly cut from heat-treated bar, mechanically polished to remove the surface oxide layer and ultrasonically cleaned with acetone in order to maintain alloy surface finish. The received alloy as referential material was experienced the same heat treatment in vacuum furnace. The specimens were hydrogenated by holding them at 750 °C in pure hydrogen atmosphere for 2 h and then air-cooled to room temperature. After hydrogenation, the hydrogen content of specimens was measured by weighting specimens before and after hydrogenation treatment using electronic balance with accuracy of 10^{-5} g . Specimens with various amounts of hydrogen were attained by controlling hydrogen pressure. Dehydrogenation process was carried out by vacuum annealing heat treatment. Hydrogenated specimens were held at 750 °C in vacuum furnace until vacuum level reached to 10^{-3} Pa . After dehydrogenation, hydrogen content was measured by hydrogen-oxygen analyzer.

All metallographic specimens were mechanically polished with sandpaper, then etched using a solution of $V(\text{HF}):V(\text{HNO}_3):V(\text{H}_2\text{O})=1:3:7$. Microstructure of TC21 alloys with different hydrogen contents was observed using optical microscopy (OM) and scanning electron microscopy (SEM, S-5200). Micro-hardness was tested by micro hardness tester (MVS-1000JM2T) with a dwell time of 10 s and load of 4900 mN. Phases of hydrogenated TC21 alloys were measured by XRD which was performed via RINT 2100 X-ray diffraction instrument with Cu K_α radiation under 40 kV and 20 mA, scanning parameter of $0.006^\circ/\text{step}$. Thin foils for transmission electron microscopy (TEM) analysis were electro-polished by MTP-1A twin-jet electro-polisher in a solution bath consisting of CH_3OH , $\text{C}_4\text{H}_9\text{OH}$ and HClO_4 (volume ratio of 10:6:1). Thin foils were observed using JEOL-JEM 3010 TEM instrument at 300 kV.

3 Results and discussion

3.1 X-ray diffraction analysis

XRD patterns of TC21 alloys before and after hydrogenation with different hydrogen contents are shown in Fig. 1. As seen from the XRD patterns, as-received TC21 alloy consists of primary α phase and a small amount of β phase. After hydrogenation, XRD patterns change apparently. The intensity of α phase decreases with the increase of hydrogen content, and even some peaks with high angle disappear when hydrogen content increases to 0.576% (mass fraction) or higher, while the intensity of β phase increases with the increase of hydrogen content. Hydrogen is β phase alloying element which can reserve more β phase to room temperature during cooling. In addition, the peaks of α phase and β phase shift to low angle because the addition of hydrogen leads to expansion of lattice parameter. It is seen that some peaks of α phase and β phase are broadened due to the precipitation of face-cubic δ hydride and the generation of dislocation and twins. As hydrogen content reaches to 0.576%, some new peaks appear. From PDF card and TEM investigation discussed later, new phase is face-cubic δ hydride with molecular formula of TiH_x ($1.5 < x < 2$) and CaF_2 type structure.

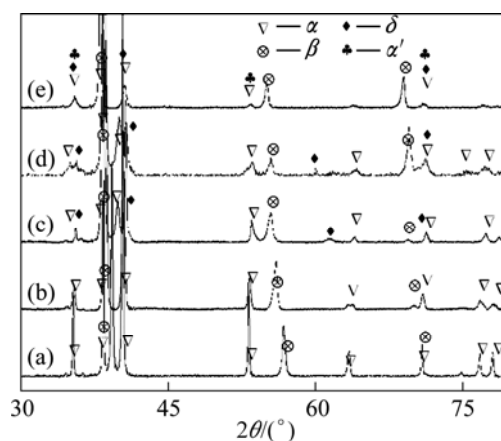


Fig. 1 XRD patterns of hydrogenated TC21 alloys with different hydrogen contents: (a) As-received; (b) 0.196% H; (c) 0.438% H; (d) 0.576% H; (e) 1.028% H

3.2 Microstructure of hydrogenated TC21 alloys

Figure 2 shows the microstructures of as-received and hydrogenated TC21 alloy with different hydrogen contents. It is seen that the as-received one has equiaxed α phase (white) and transformed β phase (dark) with lamellar α beam domain (Fig. 2(a)). With the addition of hydrogen, α phase and β phase boundaries become ambiguous (Fig. 2(b)). Compared with the as-received one, the contrasts of equiaxed α phase and transformed β

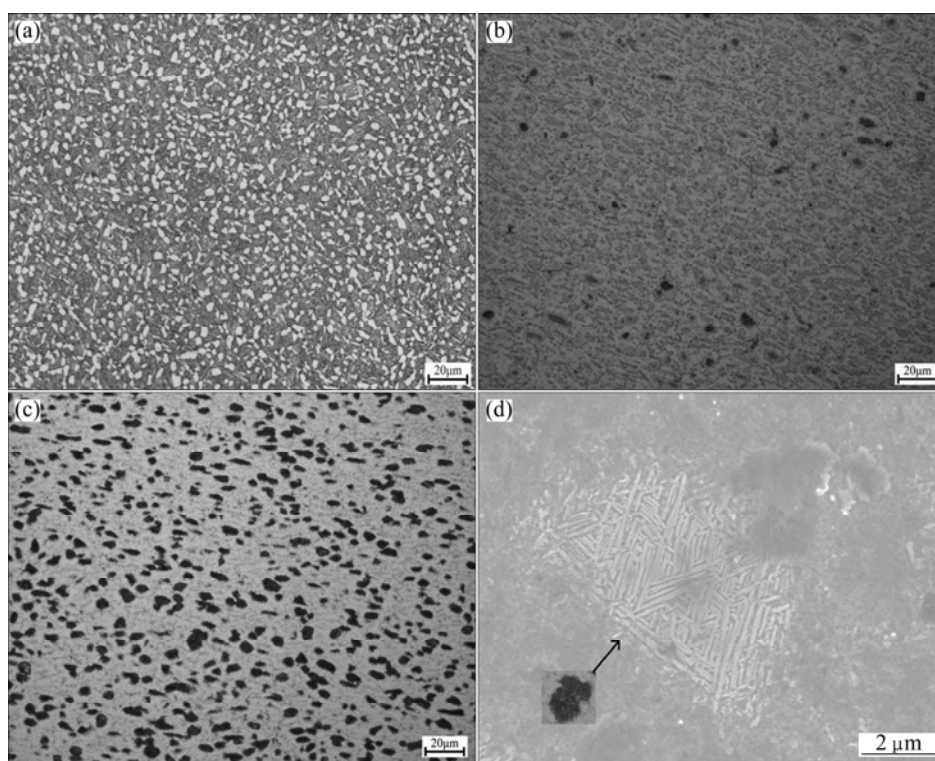


Fig. 2 Microstructures of hydrogenated TC21 alloys with different hydrogen contents: (a) As-received; (b) 0.576% H; (c, d) 1.028% H

phase under optical microscopy with 1.028% H are completely reversed (Fig. 2 (c)). The dark phase in TC21 alloy with 1.028% H was analyzed by SEM, as shown in Fig. 2(d). Lamellar structure is observed in dark phase. Several lamellar structures with similar length are distributed parallel and constructed colonies with different orientations. The growth of lamellar structure is restricted each other. The reason is that hydrogen causes the decrease of relative electrochemical potential of equiaxed α phase and transformed β phase. Hydrogen as β stabilizing element increases electrochemical potential of β phases when hydrogen atoms exist in interstitial sites of β phases. However, the change of lattice volume in α phase leads to the elastic or plastic strain in matrix. The formation of lattice defects decreases electrochemical potential of α phase. The critical value of hydrogen content is 0.5%–0.6%.

3.3 TEM analysis

TEM micrographs of the hydrogenated TC21 alloys are shown in Figs. 3 and 4. The selected area electron diffraction (SAED) pattern does reveal the presence of FCC- δ titanium hydride, as shown in Fig. 3(c) and Fig. 4(a). The bright field micrographs show that lamellar δ hydrides precipitate not only from α phase, but also from β phase. The lamellar δ hydrides are approximately parallel and distributed alternatively with lamellar α' phase. And HCP α' martensite with different orientation

is detected in the specimen (Fig. 3(a)). A large number of twins arise (Figs. 4(a) and (c)). In addition, some particles precipitate in the specimen with 1.028% hydrogen (Fig. 4(c)). According to SAED pattern, the particle is Ti_3Al phase with HCP structure (Fig. 4(d)) because of redistribution of alloying elements in α and β phases. The amount of Al in α phase increases with the increase of hydrogen added, and Ti_3Al phase precipitates when Al element in α phase exceeds the limitation.

Microstructures of TC21 alloy with different hydrogen contents were studied. As seen from the results of OM, XRD and TEM analysis, the addition of hydrogen results in obvious change of microstructure, and accelerates the generation of twin and the precipitation of Ti_3Al phase. The formation of hydrides and twin is discussed as follows.

WANG et al [16] indicated that the hydrogen absorption process obeyed three-dimension diffusion mechanism and the formation of hydride proceeded through atom diffusion. The reasons are as follows: 1) Considerable diffusivity of hydrogen in titanium alloys can not be ignored. Diffusion coefficient of hydrogen in pure titanium was described by WASILEWSKI and KEHL [17] as: $D_{\alpha}=1.8 \times 10^{-2} \exp((-6200 \pm 340)/T)$, $D_{\beta}=1.95 \times 10^{-3} \exp((-3320 \pm 250)/T)$, where D_{α} is the diffusivity of hydrogen in α phase, D_{β} is the diffusivity of hydrogen in β phase and T is the temperature; 2)

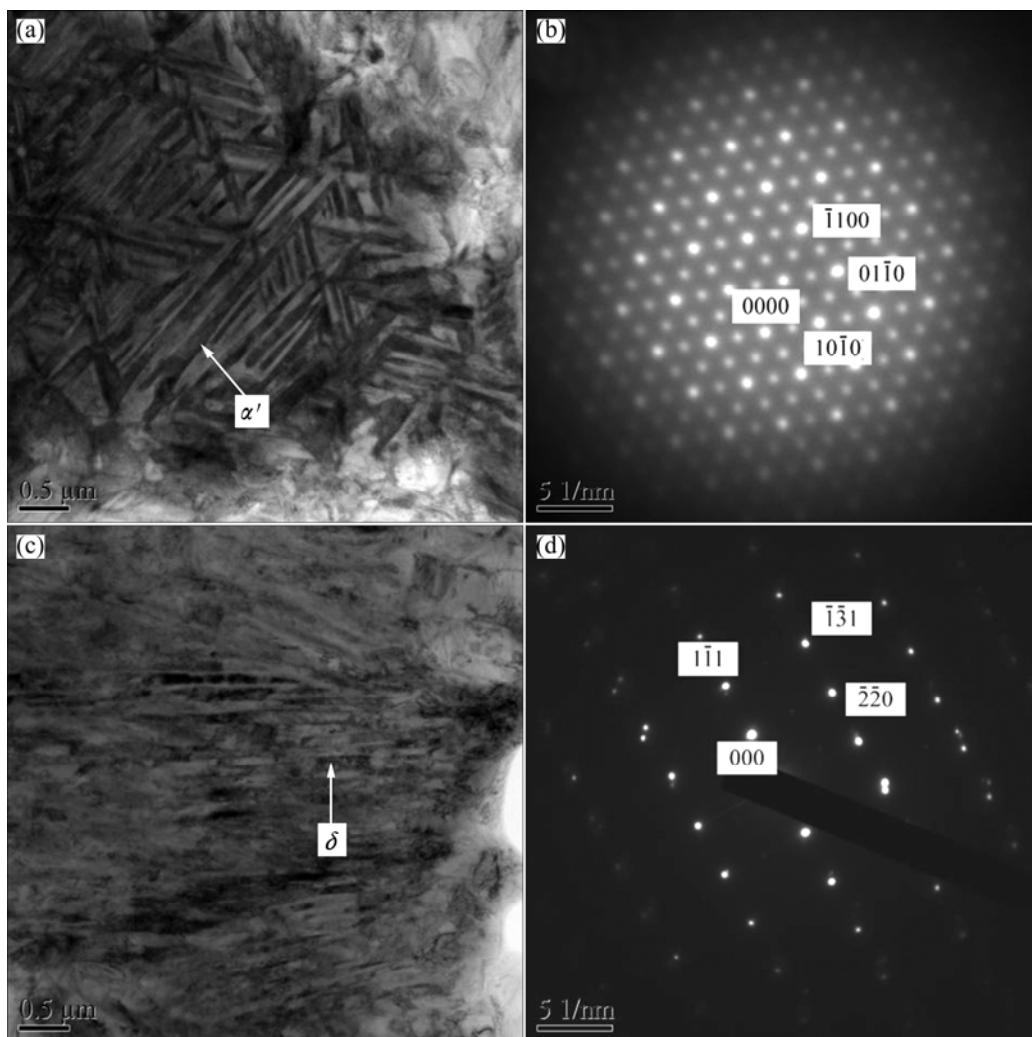


Fig. 3 TEM images of TC21 alloy with 0.576% hydrogen: (a) α' martensite; (b) SEAD pattern of α' martensite; (c) δ hydride; (d) SEAD pattern of δ hydride

hydrogen weakens the bonding force of atoms and increases the diffusivity of alloying elements; 3) the crystal structures between hydride and parent phase are different and the shear mechanism can not be realized.

A lot of dislocations were observed in α phase. Hydrogen atoms aggregated at dislocation and distortions were created in α phase. Dislocation supplied bulk of nucleation sites for hydrides and distortion energy facilitated the growth of hydrides. The solubility of hydrogen in β phase at high temperature was large and decreased with the decrease of temperature. The saturation state appeared and $\beta_{\text{H}} \rightarrow \alpha + \delta$ eutectoid reaction occurred at eutectoid temperature.

According to the investigation of TEM, bulk of twins was observed in hydrides when the hydrogen content was high, where twin plane was $\{110\}$ and zone axis was $[011]_{\delta}$. This kind of twin appears as parallel and regular array of annealing twins due to eutectoid ($\beta \rightarrow \alpha + \delta$) change.

3.4 Microhardness of TC21 alloys with different hydrogen contents

Microhardness depends on the composition and microstructure, and it is a simple way to represent the effect of hydrogen on phase transformation of titanium alloys. Microhardness variation of TC21 alloys with different hydrogen concentration is shown in Fig. 5. As hydrogen content increases, the microhardness decreases abruptly, reaches a minimum value when hydrogen content is 0.5%–0.6%, and then increases slightly. According to XRD analysis, the proportion of β phase which is softer than α phase increases with the addition of hydrogen because hydrogen lowers β transus temperature. Moreover, the addition of hydrogen changes elastic moduli and dislocation slip systems that are activated, which accelerates dislocation motion. Therefore, the microhardness decreases when hydrogen content increases. When the addition of hydrogen exceeds solid solubility limit, brittle phase of hydrides will precipitate. According to TEM images (Figs. 4 (a)

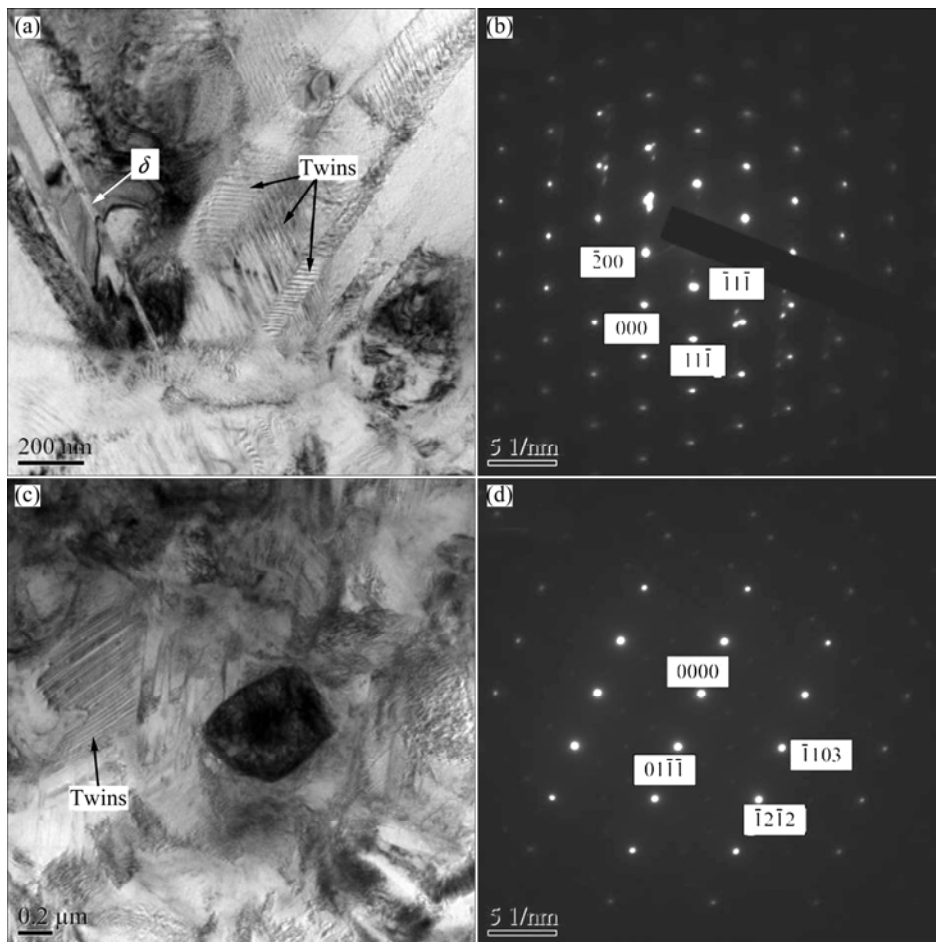


Fig. 4 TEM images of TC21 alloy with 1.028% hydrogen: (a) δ hydride; (b) SEAD pattern of δ hydride; (c) Ti_3Al phase; (d) SEAD pattern of Ti_3Al phase

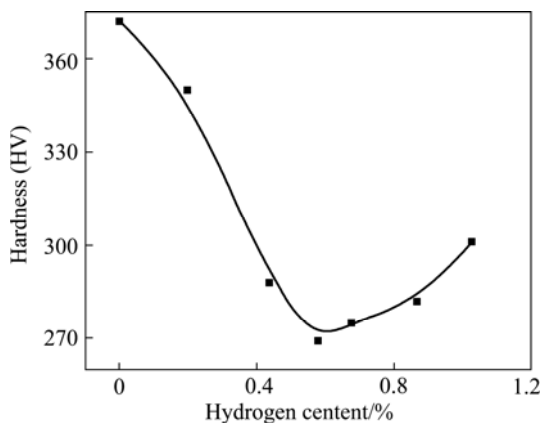


Fig. 5 Microhardness of TC21 alloys with different hydrogen contents

and (c)), bulk of twins is formed. Hence, as microhardness reaches a minimum, it increases slowly.

3.5 Phases and microstructure of dehydrogenated TC21 alloy

XRD patterns of hydrogenated and dehydrogenated TC21 alloy with hydrogen content of 1.028% are shown in Fig. 6. As shown in Fig. 6, the dehydrogenated TC21 alloy shows similar peaks with the as-received one,

which consists of α and β phases. New peaks which result from the precipitation of hydrides and martensites disappear because of the decomposition of hydrides and the precipitation of α phase from hydrogen-rich β phase.

Figure 7 shows the microstructure of dehydrogenated TC21 alloy, which consists of equiaxed α phase and transformed β phase. Compared with the as-received one, lamellar α phase precipitated from β -rich phase. The equiaxed dark phases of TC21 alloy with 1.028% hydrogen consist of bulk lamellar structure and twins. A large number of α phase nucleates at twins and phase boundary during dehydrogenation. Moreover, lack of hydrogen leads to the increase of transformation temperature. According to lever law and phase equilibrium law, lamellar α phase precipitates from β phase.

3.6 Microstructure evolution mechanism of TC21 alloy during hydrogenation and dehydrogenation

Limited solubility of hydrogen in α and β phases has great difference, and the effects of hydrogen on phase transformation of α and β phases are different. According to different action of hydrogen, phase

transformation of α and β phases during hydrogenation and dehydrogenation is shown in Fig. 8. α phase: $\alpha \rightarrow \alpha_H \rightarrow \alpha_H + \beta_H \rightarrow \alpha + \delta + \alpha' \rightarrow \alpha$; β phase: $\beta \rightarrow \beta_H \rightarrow \alpha + \delta + \beta_H \rightarrow \alpha + \beta$.

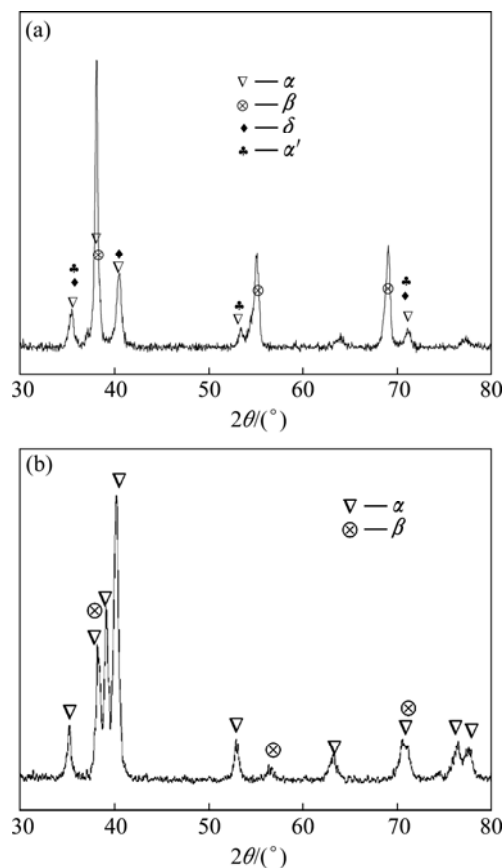


Fig. 6 XRD patterns of hydrogenated (a) and dehydrogenated (b) TC21 alloy with 1.028% hydrogen

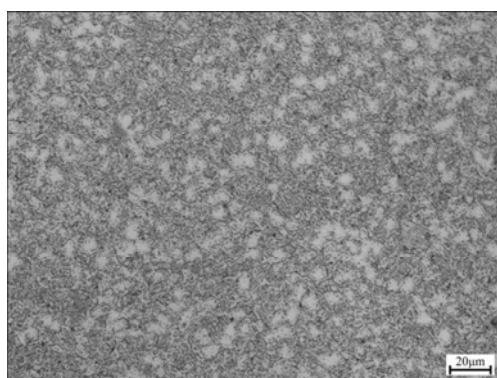


Fig. 7 Microstructure of dehydrogenated TC21 alloys with 1.028% hydrogen

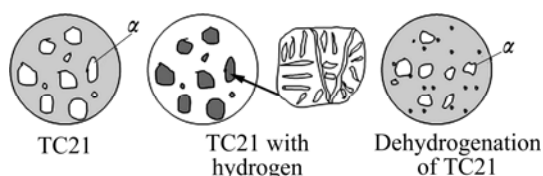


Fig. 8 Microstructure evolution of TC21 alloys during hydrogenation and dehydrogenation

4 Conclusions

1) The microstructural evolution and phase transformation of hydrogenated and dehydrogenated TC21 alloys were investigated. After hydrogenation, the microstructure of TC21 alloy changed evidently. The contrasts of equiaxed α phase and transformed β phase under optical microscope were reversed when hydrogen content exceeded critical value (0.5%–0.6%). White α phase shifted to dark phase, and lamellar structure in dark structure was observed by SEM. α' martensite, δ hydride and particles were determined by XRD, SEM and TEM analyses.

2) Bulk of twin was observed. With the increase of hydrogen content, the microhardness of hydrogenated TC21 alloy decreased, reached a minimum value at 0.5%–0.6% H, and then increased slightly. The critical hydrogen content of minimum hardness is consistent with the fact that the contrast of equiaxed α phase and transformed β phase changes.

References

- [1] FEI Yu-huan, ZHOU Lian, QU Heng-lei, ZHAO Yong-qing, HUANG Chuan-zhen. The phase and microstructure of TC21 alloy [J]. *Mater Sci Eng A*, 2008, 494: 166–172.
- [2] WANG Yi-hong, KOU Hong-chao, CHANG Hui, ZHU Zhi-shou, SU Xiao-fan, LI Jin-shan, ZHOU Lian. Phase transformation in TC21 alloy during continuous heating [J]. *J Alloys Compd*, 2009, 472: 252–256.
- [3] WANG Yi-hong, KOU Hong-chao, CHANG Hui, ZHU Zhi-shou, ZHANG Feng-shou, LI Jin-shan, ZHOU Lian. Influence of solution temperature on phase transformation of TC21 alloy [J]. *Mater Sci Eng A*, 2009, 508: 76–82.
- [4] SENKOV O N, QAZI J I, FRONES F H. Recent advances in the thermohydrogen processing of titanium alloys [J]. *JOM*, 1996, 48: 42–47.
- [5] SENKOV O N, FRONES F H. Thermohydrogen processing of titanium alloys [J]. *Int J Hydrogen Energy*, 1999, 24: 565–576.
- [6] FROES F H, SENKOV O N, QAZI J I. Hydrogen as a temporary alloying element in titanium alloys, thermohydrogen processing [J]. *Int Mater Rev*, 2004, 49: 227–245.
- [7] ZONG Y Y, SHAN D B, LÜ Y, GUO B. Effect of 0.3 wt%H addition on the high temperature deformation behaviors of Ti–6Al–4V alloy [J]. *Int J Hydrogen Energy*, 2007, 32: 3936–3940.
- [8] CHEN Ye-xin, WAN Xiao-jing, LI Fang, WANG Qing-jiang, LIU Yu-yin. The behavior of hydrogen in high temperature titanium alloy Ti-60 [J]. *Mater Sci Eng A*, 2007, 466: 156–159.
- [9] HE W J, ZHANG S H, SONG H W, CHENG M. Hydrogen-induced hardening and softening of a β -titanium alloy [J]. *Scripta Mater*, 2009, 61: 6–19.
- [10] WANG Xiao-li, ZHAO Yong-qing, HOU Hong-liang, WANG Yao-qi. Effect of hydrogen content on superplastic forming/diffusion bonding of TC21 alloys [J]. *J Alloys Compd*, 2010, 503: 151–154.
- [11] ZONG Ying-ying, LIANG Ying-chun, YIN Zhong-wei, SHAN De-bin. Effects of hydrogen addition on the high temperature deformation behavior of TC21 titanium alloy [J]. *Int J Hydrogen Energy*, 2012, 37: 13631–13637.

- [12] LIU H J, ZHOU L, LIU P, LIU Q W. Microstructural evolution and hydride precipitation mechanism in hydrogenated Ti-6Al-4V alloy [J]. Int J Hydrogen Energy, 2009, 34: 9596–9602.
- [13] LUO Liang-shun, SU Yan-qing, GUO Jing-jie, FU Heng-zhi. Formation of titanium hydride in Ti-6Al-4V alloy [J]. J Alloys Compd, 2006, 425: 140–144.
- [14] ZHU Tang-kui, LI Miao-quan. Effect of 0.770 wt%H addition on the microstructure of Ti-6Al-4V alloy and mechanism of δ hydride formation [J]. J Alloys Compd, 2009, 481: 480–485.
- [15] SHAN D B, ZONG Y Y, LU T F, LV Y. Microstructural evolution and formation mechanism of FCC titanium hydride in Ti-6Al-4V-xH alloys [J]. J Alloys Compd, 2007, 427: 229–234.
- [16] WANG Xiao-li, ZHAO Yong-qing, ZENG Wei-dong, HOU Hong-liang, WANG Yao-qi. Kinetics of hydrogen absorption/desorption in TC21 alloy [J]. Journal of Alloys and Compounds, 2010, 490: 531–536.
- [17] WASILEWSKI R J, KEHL G L. Diffusion of hydrogen in titanium [J]. Metallurgia, 1954, 50: 225–227.

TC21 合金吸氢与放氢后的微观组织

王小丽¹, 赵永庆², 魏晓伟¹, 侯红亮³

1. 西华大学 材料科学与工程学院, 成都 610039;
2. 西北有色金属研究院, 陕西 710016;
3. 北京航空制造工程研究所, 北京 100024

摘要: 利用光学显微镜(OM)、X 射线衍射(XRD)和透射电子显微镜(TEM)研究 TC21 合金吸氢与放氢后的组织演变和相的转变。研究表明: 吸氢后, α 和 β 相的衍射峰向低的 2θ 角方向偏移, 说明氢原子固溶于合金中, 使其晶体结构发生膨胀; TC21 合金的组织也发生明显的变化。吸氢后, α 相和 β 相的明暗对比度发生变化, 原白色 α 相(金相组织)转变为黑色, 而且黑色组织中分布有取向不同且平行排列的片状组织。XRD 分析和 TEM 观察发现, 在合金中有氢化物和 α' 马氏体生成, 还在相内和相间存在大量的孪晶和少量的粒子。这意味着氢导致 α 和 β 相中合金元素的再分配。放氢后, TC21 合金的组织与吸氢前合金的组织相似, 只包括 α 相和 β 相。

关键词: δ 氢化物; Ti_3Al 相; α' 马氏体; 孪晶

(Edited by Chao WANG)